Radiation Oncology

RESEARCH

Open Access

High incidence of radiation-induced brain necrosis in the periventricular deep white matter: stereotactic radiotherapy for brain metastases using volumetric modulated arc therapy

Takayuki Ohguri[1*], Hirohide Itamura[1], Subaru Tani[1], Eiji Shiba[1] and Junkoh Yamamoto[2]

Abstract

Purpose In this retrospective study, we aimed to evaluate the efficacy and incidence of radiation-induced brain necrosis (RBN) after volumetric modulated arc therapy-based stereotactic irradiation (*VMAT-STI*) for brain metastases.

Methods In the 220 brain metastatic lesions included between January 2020 and June 2022, there were 1–9 concurrently treated lesions (median 1). A biologically effective dose *(BED)10* of 80 Gy and a reduced BED10 of 50 Gy were prescribed to the gross tumor volume (GTV) and planning target volume *(PTV) (PTV = GTV + 3 mm)* margins, respectively. The number of fractions was adjusted from 3 to 15 to accommodate different GTV sizes; for larger tumor volumes, this was increased while maintaining the BED10 values comparable to those for GTV and PTV margins.

Results Of the total patients, 16 (7%) exhibited locally progressive lesions; local tumor recurrence was observed in 2 (1%) patients, while RBN was noted in 14 (6%) patients. RBN was significantly more prevalent in the deep white matter around the lateral ventricles (DWM-LV) than in other sites, occurring in 9/22 (41%) lesions of metastases in the DWM-LV. The 2-year actuarial incidence risk of developing RBN was significantly higher in the DWM-LV (69%) than at other sites (5%).

Conclusion The recurrence rate of brain metastases was low, and the incidence of RBN was lower in tumor sites other than the DWM-LV. However, the frequency of RBN was significantly higher in the DWM-LV region. Additional VMAT-STI-prescribed dose protocols are necessary to reduce RBN incidence in DWM-LVs.

Keywords Radiation-induced brain necrosis, Stereotactic radiotherapy, Volumetric modulated arc therapy

*Correspondence:
Takayuki Ohguri
ogurieye@med.uoeh-u.ac.jp
[1]Department of Therapeutic Radiology, Hospital of the University of Occupational and Environmental Heath, Kitakyushu, Japan
[2]Department of Neurosurgery, School of Medicine, University of Occupational and Environmental Health, Kitakyushu, Japan

Introduction

Recent advances in cancer treatment have improved the prognosis of patients with advanced cancer, and radiotherapy for brain metastases is required to provide long-term tumor control and safety. In stereotactic radiotherapy using linear accelerators, volumetric modulated arc therapy (VMAT)-based stereotactic radiotherapy (VMAT-STI) has become popular, allowing a more detailed setting of the dose to the normal brain surrounding the tumor and a dose increase inside the tumor, compared with conventional stereotactic radiotherapy using three-dimensional (3D) irradiation. However, the differences in the risk of radiation brain necrosis (RBN) and the optimal dose for each region of the brain are unknown, and uniform treatment is often applied regardless of the metastatic site. Previous animal and human studies have demonstrated that white matter is more susceptible to radiation-induced damage than gray matter, increasing the risk of RBN [1–3].

Compared with conventional 3D irradiation and fixed gantry IMRT, VMAT-STI allows for more detailed dose settings from the tumor center to the periphery and can treat multiple brain metastases in a shorter irradiation time. In single-fraction stereo-tactic radiosurgery (SRS), the incidence of symptomatic brain necrosis exceeds 20% when the V12 Gy volume surpasses 5–10 mL [4]. Furthermore, even when the gross tumor volume (GTV) margin dose is reduced to 18 Gy (BEDGy10 of 50 Gy), there re-mains a risk of developing RBNs in tumors of > 2 cm in diameter [4]. Although microscopic infiltration of brain metastases into the surrounding brain tissue is typically estimated to be 1 mm, intraoperative fluorescence diagnosis and pathology reports have documented cases with infiltration depths of ≥ 2–3 mm (2, 3) [5, 6]. Notably, larger brain metastases tend to exhibit deeper invasion of the surrounding brain tissue. Based on these findings, Ohtakara et al. proposed a VMAT-STI protocol utilizing separate prescription doses for the GTV margin and a prophylactic margin of GTV + 2–3 mm [7, 8]. To mitigate the risk of RBN, the protocol also incorporated an increased number of fractions for larger tumor volumes, while maintaining BEDGy10 doses equivalent to both the GTV margin and GTV + 2–3 mm.

In this study, we employed a VMAT-STI protocol involving precise dose and fractionation specifications within, at the limbus of, and surrounding the GTV to treat brain metastases. To the best of our knowledge, there is limited literature on the efficacy of VMAT-STIs with detailed dosimetry as well as on the incidence and risk factors associated with brain necrosis. This study aimed to evaluate the efficacy and toxicity of VMAT-STIs for brain metastases, and the incidence of RBN in relation to the metastatic site.

Materials and methods

Patients

From January 2020 to June 2022, patients with brain metastases were prospectively enrolled in the radiotherapy database at the authors' institution. During the same period, consecutive patients with brain metastases were treated using VMAT-STI. There were 220 brain metastases in 63 patients treated with VMAT-STIs. The inclusion criteria were as follows: (i) patients with metastatic brain tumor(s) treated with VMAT-STI and pathologically confirmed primary malignant tumors, and (ii) patients who had under-gone at least one contrast-enhanced MRI scan 1 month after the end of irradiation. Patient characteristics are shown in Table 1. Written informed consent for the treatment was obtained from all patients. This study was approved by institutional review board of the authors (protocol code UOEHCRB22-078).

VMAT-STI protocol

VMAT-STI was performed using a linear accelerator (Elekta, Versa HD™). The patients were imaged using high-resolution thin-slice (1.0–2.0 mm) computed tomography (CT) and immobilized in the supine position using a thermoplastic head-mask fixation system. The treatment plans were implemented using Monaco™ (Elekta) in all patients. GTV was contoured using the fusion of CT images for treatment planning and contrast-enhanced MRI. Figure 1 shows a schematic representation of the VMAT-STI protocol for brain metastases. BED10 = 80 Gy was prescribed as the GTV marginal dose, and the marginal dose of the PTV (GTV + 3 mm) was reduced to BED10 = 50 Gy. The central dose of the tumor was increased to more than 125% of the marginal GTV. The number of fractionations was adjusted between 3 and 15 depending on the GTV size. For larger tumor volumes, the number of irradiation fractions increased, and the BED10 values of the GTV margins and GTV + 3 mm were comparable. The relationship between the number of dose fractions and tumor volume is shown in Table 1.

Evaluation of the metastatic sites and RBN

Metastatic sites were classified into the following areas based on anatomical regions observed on MRI images: brain cortical and/or subcortical white matter (BC/SCWM); deep white matter around the lateral ventricles (DWM-LV), defined as lesions bordering the lateral ventricles or located in the deep white matter within 10 mm of their perimeter; and cerebellum, basal ganglia, thalamus, midbrain, and hippocampus.

Assessments using enhanced MRI or CT were scheduled before treatment and every 1–6 months after treatment until treatment failure or death. Local tumor recurrence was assessed using the RANO-BM (Response Assessment in Neuro-Oncology-Brain Metastases)

Table 1 Patient characteristics

Characteristics	n
No of patients	63
No of treated metastases	220
No of STI courses	98
Patients with one STI course	41
Patients with 2 STI courses	13
Patients with 3 STI courses	6
Patients with 4 STI courses	2
Patients with 5 STI courses	1
No of treated metastases in each course	
1	48
2	25
3	9
4	3
5	5
6	3
7	4
12	1
Age (median, range)	70 (42-86)
Sex	
Male/female	31/32
Primary lesion	
Lung cancer	
NSCLC	32
SCLC	9
Breast cancer	13
Malignant melanoma	3
Others	6
VMAT-STI	
Total dose*/fractions	
36 Gy/3 fractions	64
Maximum tumor volume (cc)	0.2 (0.02-1.5)
Median tumor volume (cc)	0.1 (0.02-1.4)
43 Gy/5 fractions	17
Maximum tumor volume (cc)	1.5 (0.06-5.8)
Median tumor volume (cc)	0.7 (0.04-2.8)
50 Gy/8 fractions	2
Maximum tumor volume (cc)	1.9 (1.7-2.0)
Median tumor volume (cc)	1.9 (1.7-2.0)
53Gy/10 fractions	14
Maximum tumor volume (cc)	3.4 (0.5-10.3)
Median tumor volume (cc)	2.0 (0.5-9.4)
59Gy/15 fractions	1
Maximum tumor volume (cc)	12
Median tumor volume (cc)	12

*GTV marginal dose
NSCLC; non-small cell lung cancer, SCLC; small cell lung cancer, VMAT-STI; volumetric modu-lated arc therapy-based stereotactic irradiation, GTV; gross tumor volume.

guidelines [9]. Locally progressive lesions of the treated lesion(s) were classified as RBN or tumor recurrence. The diagnosis of RBN and tumor recurrence was confirmed based on temporal MRI images and by considering the me-thionine PET images, the changes in tumor markers in some cases, and pathological findings on excised specimens. Local control rate was defined as the period during which there were no local progressive lesions.

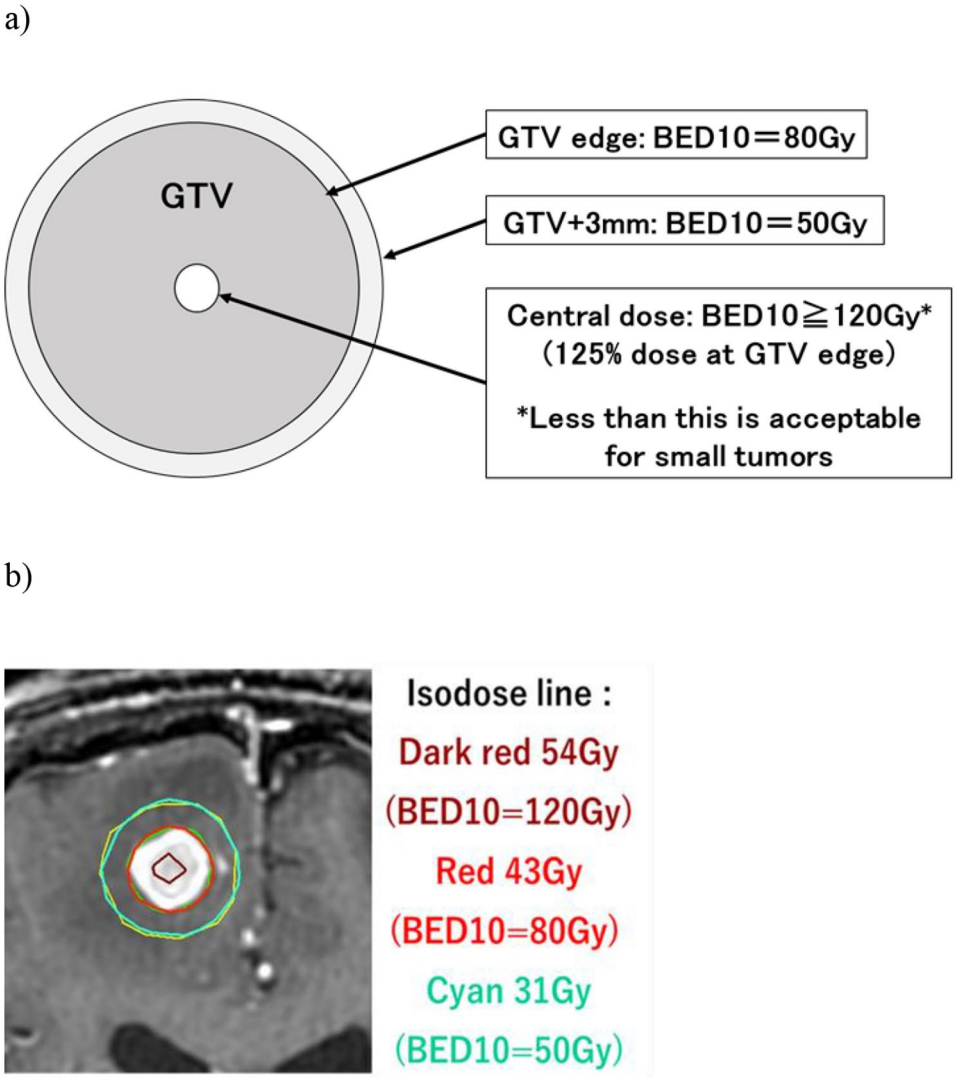

Fig. 1 VMAT-STI protocol for brain metastases. **a**) Schematic diagram. **b**) Example of STI plan-ning with VMAT. Biologically Effective Dose (BED10) of 80 Gy (as red line of 43 Gy in 5 fractions in this case) is matched to the GTV marginal dose (as green line). BED10 of 50 Gy (as cyan line of 31 Gy in 5 fractions in this case) is matched to the PTV (GTV + 3 mm as yellow line). Tumor center dose is increased to at least 125% of the GTV marginal dose (as dark red line of 54 Gy in 5 fractions in this case)

The analyses of certain factors for developing RBN were investigated using Fisher's exact probability or Mann–Whitney U test. Local control and incidence rates of devel-oping RBN were calculated from the first day of VMAT-STI using the Kaplan–Meier method. Statistical significance of the differences between the actuarial curves was assessed using the log-rank test.

Overall survival was defined as the time from the last day of the first VMATSTI course to death. Distant brain progression-free survival (DPFS) was defined as the time from the last day of the first VMATSTI course to the occurrence of distant brain failure, as indicated by the appearance of new or progressive brain metastases outside the PTV or death.

Results

Local tumor recurrence and RBN

Locally progressive lesions were observed in 16 (7%) of the 220 brain metastases treated with VMAT-STI, and local tumor recurrence of the treated brain metastases was observed in 2 (1%) of the 220 brain metastases and 2 (%) of the 63 patients. RBN was recognized in 14 (6%) of the 220 patients with brain metastases and 14 (22%) of the 63 patients. Table 2 presents the clinical details of the 16 locally progressive lesions. Local tumor recurrence was observed only in two brain metastases. Both lesions had a large tumor volume (9.7 cc and 11.9 cc) and underwent tumor removal.

Fourteen (88%) of the sixteen locally progressive lesions were diagnosed as RBN based on clinical

Table 2 Clinical details of the 16 local progressive lessions

Case No.	Age in years	Sex	Site	Primary lesion	Tumor volume (cc)	Total dose/fractions	Time to onset of RBN (months)	Symptoms	Treatments (drug, starting dose of steroids /body and total duration of steroid administration)
RBN									
1	53	F	DWM-LV	Breast	0.1	36Gy/3	14	Agraphia	Betamethasone, 4mg, 23 mos.
2	65	F	DWM-LV	Lung	0.5	36Gy/3	16	Dizziness	Betamethasone, 1mg, 12 mos.
3	62	M	DWM-LV	Lung	0.7	43Gy/5	25	Spasm	Antiepileptic drug
4	69	M	DWM-LV	Lung	1	36Gy/3fractions	19	None	Betamethasone, 0.5mg, 11 mos.
5	42	M	DWM-LV	Lung	1.7	43Gy/5fractions	23	None	Betamethasone, 1mg, 15 mos.
6	70	M	DWM-LV	Lung	3.5	53Gy/10fractions	9	None	Betamethasone, 2mg, 7 mos.
7	61	F	DWM-LV	Breast	0.6	36Gy/3fractions	16	None	Dexamethasone, 2mg, 6 mos.
8	64	F	DWM-LV	Lung	0.1	36Gy/3fractions	6	None	None
9	72	M	DWM-LV	Lung	0.4	53Gy/10fractions	12	None	None
10	80	F	BC-frontal	Lung	4.3	53Gy/10fractions	7	Seizures	Antiepileptic drug and betamethasone, 4mg, 24 mos.
11	72	M	BC/SC-frontal	Lung	0.5	36Gy/3fractions	11	Dizziness	Betamethasone, 2mg, 24 mos.
12	68	M	BC/SC-frontal	SG	1	36Gy/3fractions	25	None	None
13	59	F	Midbrain	Breast	0.1	36Gy/3fractions	24	None	Betamethasone, 2mg, 4 mos.
14	73	F	Cerebellum	Ovary	0.1	36Gy/3fractions	14	None	None
Recurrence									
1	45	F	SC-occipital	Melanoma	9.7	53Gy/10fractions	15	Headache	Resection and WBRT
2	74	F	BC-occipital	Lung	11.9	59Gy/15fractions	18	Paralysis	Resection and RT

RBN; radiation brain necrosis, VMAT-STI; DWM-LV; deep white matter around the lateral ven-tricles, BC/SC; brain cortical and/or subcortical white matter, SG; salivary gland.

findings, including the post-onset course of the disease. The median time to RBN onset after VMAT-STI was 15 months (range, 6–25). Nine of fourteen patients with RBN were administered steroids. No patient experienced poor control with steroid therapy or required explantation. Table 3 shows the incidence of RBN after VMAT-STI for brain metastases among the metastatic sites. RBN was significantly more common in the DWM-LV than in other sites, occurring in 9 (41%) of the 22 lesions in brain metastases from the DWM-LV. The analyses of certain factors for RBN after VMAT-STI are shown in Table 4. Other factors were not significantly associated with the development of RBN. Figure 2 shows the actuarial incidence risk of developing RBN for different meta-static sites and dose fractions. The actuarial incidence risk at 2-year between in the DWM-LV and other sites was 69% and 5%, respectively, and the difference was significant (Fig. 2a, $P < 0.0001$). Case no. 2 in Table 2, which is associated with RBN, is presented in detail in Fig. 3.

Local control rate and survivals

The 3-year local control rate was 82% in all 220 patients with brain metastases (Fig. 4a). The local control rates for different radiation dose fractions are shown in Fig. 4b. There was no significant difference in the local control rates between brain metastatic lesions treated with 36 Gy/3 and 43 Gy/5 fractions. However, the brain metastatic lesions were treated with 50–59 Gy/8–15 fractions. exhibits significantly lower local control rates. The local control rate in the DWM-LV region was significantly lower than that in the other sites ($P < 0.0001$). The 3-year local control rate was 31% in DWM-LV and 89% in the other sites (Fig. 4c).

Overall survival rate and DPFS rates are shown in Fig. 4d. The 3-year overall survival rate was 52% for all 63 patients. The median overall survival time was 39.5 months. The 3-year DPFS was 17%, with a median DPFS of 7.7 months.

Table 3 Insidence of RBN after VMAT-STI for brain metastases among the metastatic sites

	With RBN (n=14) n (%)	Without RBN (n=206) n (%)
BC/SCWM	3 (2)	142 (98)
Frontal lobe	3 (6)	47 (94)
Temporal lobe	0 (0)	29 (100)
Occipital lobe	0 (0)	32 (100)
Parietal lobe	0 (0)	33 (100)
DWM-LV	9 (41)*	13 (59)
Cerebellum	1 (2)	44 (98)
Basal ganglia	0 (0)	3 (100)
Thalamus	0 (0)	2 (100)
Midbrain	1 (100)	0 (0)
Hippocampus	0 (0)	1 (100)

*p <0.001

Table 4 Analyses of certain factors for the developing RBN

	With RBN	Without RBN	
	n= 14 (%)	n=206 (%)	p
Age			0.999
Median (range)	67 (40-80)	70 (42-86)	
Tumor volume			0.169
Median (range)	0.8 (0.04-4.3)	0.16 (0.01-18.1)	
Fractionation			
36Gy/3fractions	9	129	0.999
Others	5	77	
Whole brain RT			
Yes	2	71	0.1502
No	12	135	
Sites			
DWM-LV	9	13	<0.0001
Others	6	192	

* p <0.0001 (Fisher's exact test)

Discussion

To our knowledge, this is the first study to investigate the impact of VMAT-STI treatment, characterized by a detailed dose prescription within, at the limbus, and surrounding the GTV, as well as dose fraction adjustment based on tumor size while maintaining BEDGy10, on treatment efficacy and site-specific brain necrosis incidence for brain metastasis. The strength of this study

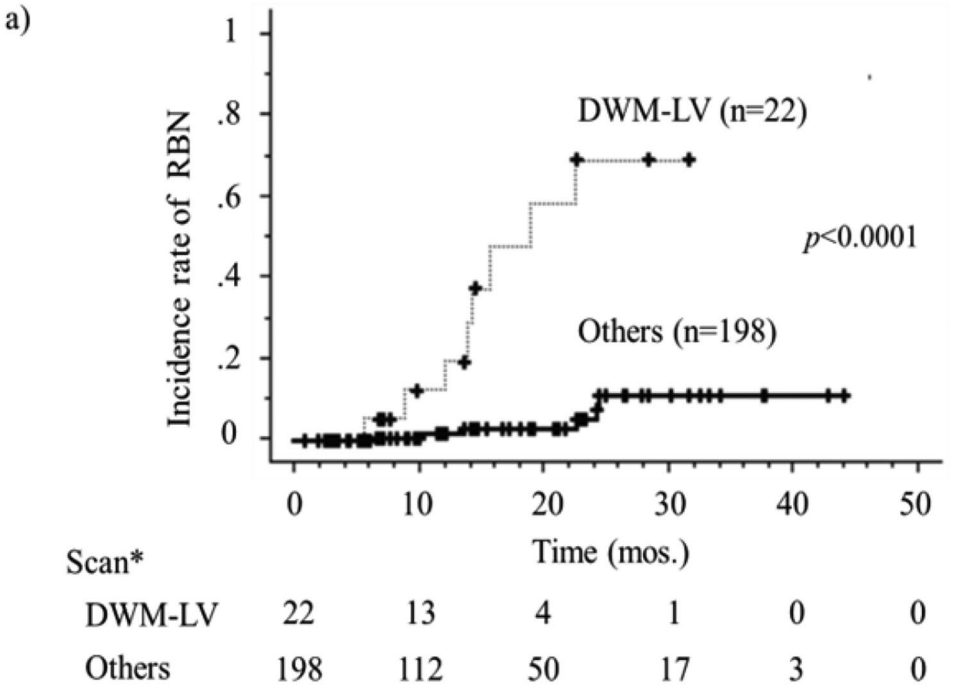

Scan*						
DWM-LV	22	13	4	1	0	0
Others	198	112	50	17	3	0

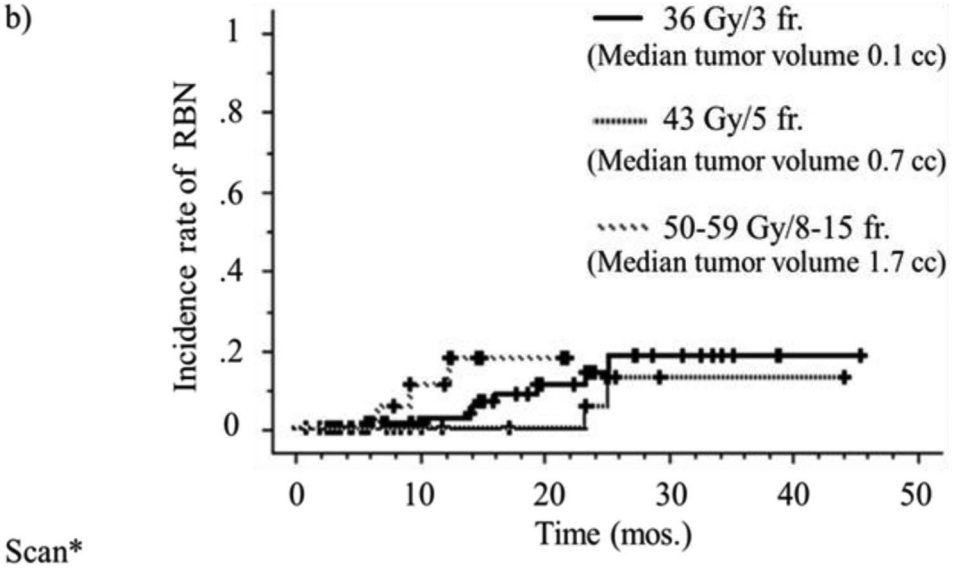

Scan*						
36 Gy/3 fr.	140	86	32	17	2	0
43 Gy/5 fr.	49	24	19	1	1	0
50-59 Gy/8-15 fr.	31	15	3	0	0	0

Fig. 2 Actuarial incidence risk of developing RBN. **a**) The incidence rate of developing RBN between DWM-LV and other sites. **b**) The incidence rate of developing RBN based on the dose fractionation

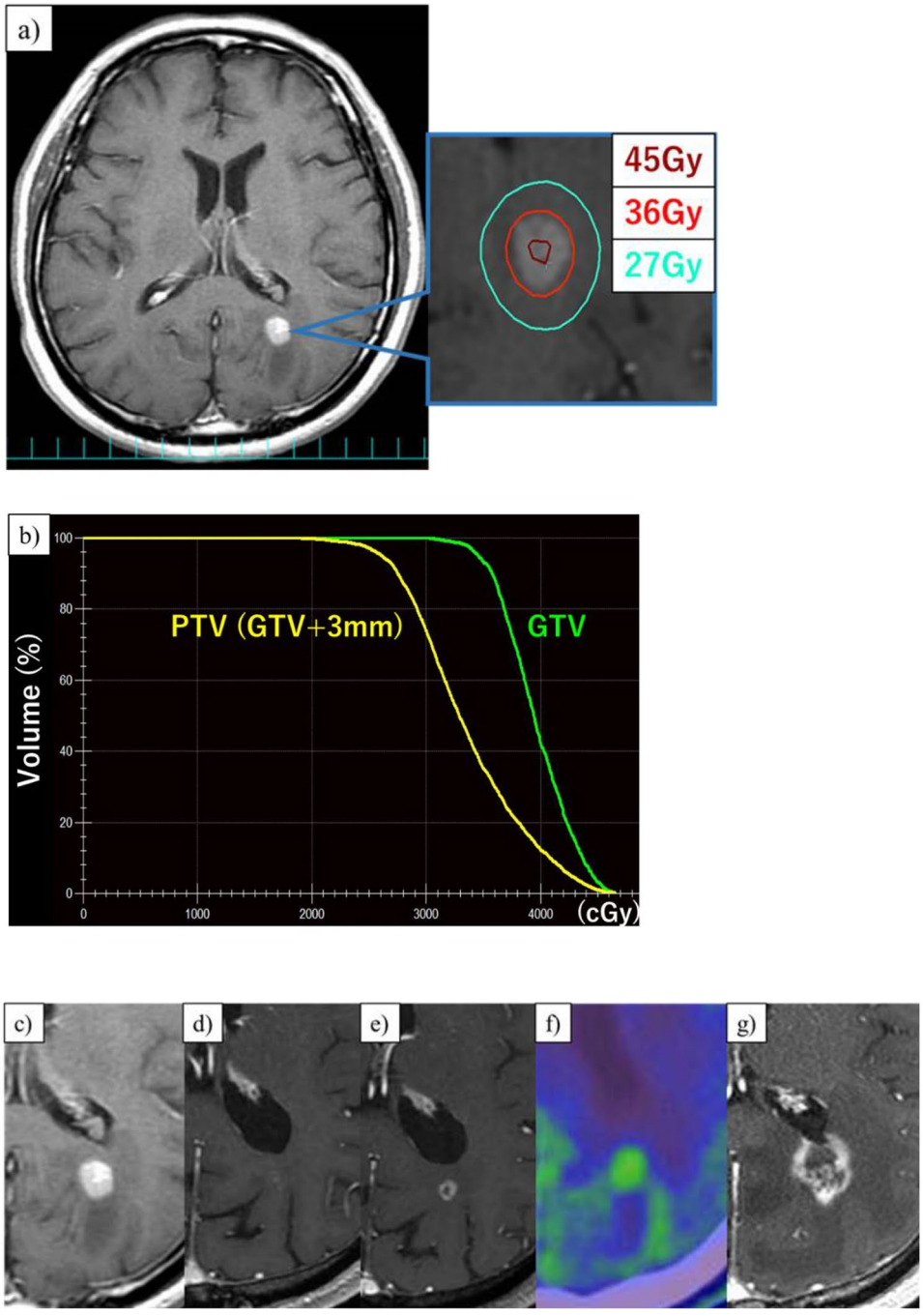

Fig. 3 Patient (no. 2 in Table 2) of radiation brain necrosis (RBN) in deep white matter around the lateral ventricle. **a**) Dose distribution diagram of stereotactic irradiation with VMAT. **b**) GTV mar-ginal dose is matched to 36 Gy in 3 fractions (red line) and GTV + 3 mm PTV marginal dose to 27 Gy (light blue line). Tumor center is increased to 45 Gy (dark red line). **b**) Dose volume histogram shows the coverage of the GTV dose, the dose reduction in the GTV + 3 mm region and the increase in the tumor center dose. Gadolinium-enhanced T1-weighted axial MR images show deep white matter brain metastasis around the lateral ventricle **c**) before stereotactic irradiation with VMAT, **d**) complete response 12 months after the stereotactic irradiation and **e**) re-growth 18 months after the stereotactic irradiation. **f**) In 11 C-methionine-PET, 20 months after the stereotactic irradiation, the re-growth lesion is lower lesion-to-brain ratio of 1.37, which is diagnostic of radiation brain necrosis. **g**) Gadolinium-enhanced T1-weighted axial MR images shows increased radiation brain necrosis 24 months after the stereotactic irradiation

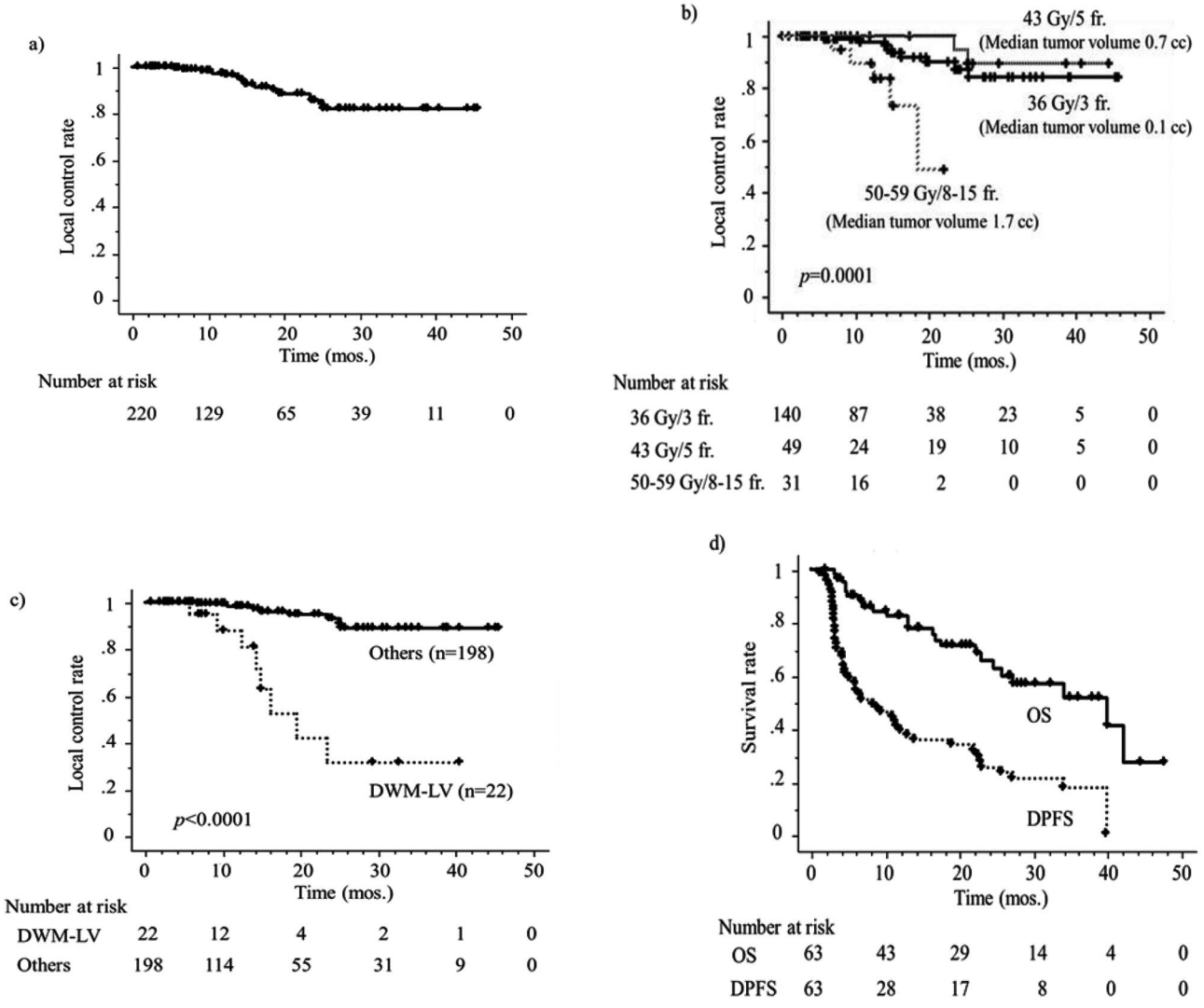

Fig. 4 The local control rate of the brain metastatses treated with VMAT-STI. **a**) The local control rate of all the 220 brain metastases. The 3-year local control rate in all the 220 brain me-tastases was 82%. **b**) The local control rate of brain metastases based on the dose fractionation. **c**) Differences in local control rates of brain metastases between DWM-LV and other sites of brain metastasis location. **d**) The overall survival rate and DPFS rates

was that it was conducted using a uniform prescription protocol. Our prescription protocol for VMAT-STIs for brain metastases showed a low incidence of tumor recurrence. However, there was a significantly higher risk of RBN only at the DWM-LV sites.

Linac-based stereotactic radiotherapy with fractionated irradiation using 3D con-formal radiation therapy has been reported to be safer than SRS, which is a single-dose irradiation. Kim et al. compared SRS and fractionated stereotactic radiotherapy (FSRT) for brain metastases and found that the incidence of toxicity was three times higher in the SRS group than in the FSRT group [10]. However, the 1-year local control rate after FSRT was only 69%, and the prescribed dose in the FSRT group (36 Gy/6 fractions, BED 58.7 Gy10) to the GTV + 1 mm margin was lower than the prescribed dose. Saito et al. reported a better 1-year local control rate of 86% with FSRT using 3D conformal radiation therapy at 35.1–37.8 Gy/3 fractions (BED 76.2–85.4 Gy10) to the GTV + 3 mm margin [11], while also noted brain necrosis in 12% of cases [12]. Our dose prescription more clearly defined the GTV margin and GTV + 3 mm doses as well as the maximum dose at the tumor center using the VMAT technique. The antitumor effect was satisfactory, with only two cases of local tumor recurrence. The incidence of brain necrosis was low at only 2.5% (5/198 lesions) of the tumor sites, except for DWM-LV. However, brain necrosis occurred significantly more frequently in the DWM-LV group (41%, 9/22). To reduce the incidence of cerebral necrosis further, we believe that it is necessary to develop a pre-scription protocol specifically for DWM-LV.

Previous studies have indicated that the risk factors for RBN in brain metastases include radiation dose, prior whole-brain radiotherapy, metastasis size, and previous surgery [13, 14]. Few studies have investigated the anatomical location of RBN. A clinical study has reported a high incidence of brain necrosis following stereotactic radiotherapy for brain metastases located in the deep white matter; in a retrospective study of 137 cases with 311 lesions treated with SRS (16–22 Gy, BEDGy10 of 41.6–70.4 Gy) for brain metastases of malignant melanoma, the overall RBN incidence was 17/137 (12.4%) [12]. The incidence of RBN in the deep white matter was 7/19 (36.8%), which was significantly higher than that in other regions. Ohtakara et al. also suggested that lesion lo-cation is important in predicting RBN after stereotactic radiosurgery, especially in depth from the brain surface [4]. Shallow lesions cause less damage to the surrounding tissues, whereas deeper lesions increase the risk of radiation injury.

Research has shown that following radiation therapy, the white matter can exhibit a range of pathological changes, including the development of small necrotic foci, vacuolation, and punctate hemorrhages [15]. The severity and progression of these lesions are influenced by factors, such as patient age and cumulative radiation dose. Over months to years, these initial changes may evolve into more extensive and severe neurodestructive lesions characterized by coagulative necrosis. This progression can lead to clinical symptoms that mimic those of recurrent intracranial neoplasms, making it challenging to differentiate radiation-induced lesions from recurrent or residual tumors using CT imaging.

Radiation preferentially damages the white matter, potentially due to direct injury to myelin and oligodendrocytes, increased vulnerability of glial cells, and exacerbated hypoxia in deep white matter regions [16]. The periventricular and deep white matter areas are particularly susceptible to ischemic changes secondary to vascular injury and may contribute to a higher incidence of RBN than other brain regions. A study in a pig model undergoing stereotactic radiosurgery revealed no obvious necrotic changes in the gray matter at doses of 80 –40 Gy [1]. Conversely, a wide range of doses from 100 –60 Gy induced necrotic changes in the white matter. Bijl et al. demonstrated significant regional differences in radiosensitivity within the rat spinal cord [2]. Specifically, the lateral white matter was more radiosensitive than the central white matter, while the gray matter exhibited high resistance to radiation. Even after a single high-dose irradiation of 80 Gy, no microscopically observable lesions were induced in the gray matter. A study investigating dose-related changes in normal brain tissue, as detected by quantitative magnetic resonance imaging following fractionated radiotherapy within the therapeutic dose range, found that dose levels exceeding 20 Gy were associated with a dose-dependent decrease in T1, which became significant 6 months post-treatment. For radiation therapy doses below 60 Gy, no significant changes in T1 were observed in the gray matter over time [3]. These studies confirm that white matter is more susceptible to radiation-induced changes than gray matter. Our research further revealed a significant increase in RBN incidence within the DWM-LV region. These results highlight the need for optimized dose prescription in VMAT-STI for brain metastases in the DWM-LV region. Specifically, increasing the number of fractions and reducing the prescribed dose to the PTV compared to current protocols may be considered.

A major limitation of this study is its retrospective design, which raises the possibility of selection bias in predictive factors. Differentiating between RBN and tumor recurrence based solely on imaging findings is challenging and potentially inaccurate. While both tumor recurrence cases in our study were confirmed through tissue resection, the RBN cases were followed up for at least three months after steroid administration, excluding the possibility of tumor recurrence. Therefore, we believe that the clinical diagnostic accuracy in our cases was maintained.

Conclusions

The antitumor effect of our VMAT-STI treatment protocol, characterized by a precise dose prescription within, at the limbus, and around the GTV as well as dose fractionation adjustment based on tumor size while maintaining BEDGy10, was satisfactory, with only two cases of local tumor recurrence. Additionally, the incidence of brain necrosis was lower at tumor sites other than the DWM-LV. However, the frequency of brain necrosis was significantly higher in the DWM-LV group, suggesting the need for a DWM-LV-specific prescription protocol to reduce the incidence of brain necrosis in these lesions.

Abbreviations

BED	Biologically effective dose
DPFS	Distant brain progression-free survival
DWM-LV	Deep white matter around the lateral ventricles
FSRT	Fractionated stereotactic radiotherapy
GTV	Gross tumor volume
OS	Overall survival
PTV	Planning target volume
RBN	Radiation brain necrosis
SRS	Single-fraction stereotactic radiosurgery
STI	Stereotactic irradiation
VMAT	Volumetric modulated arc therapy
3D	Three-dimensional

Author contributions

Conceptualization, T.O.; Data curation, T.O., H.I., S.T., and E.S.; Formal analysis, T.O. and H.I. Investigation, T.O., H.I., and S.T., Methodology, T.O.; Project administration, T.O.; Validation, T.O.; Writing—original draft, T.O. and H.I.; Writing—review and editing, T.O., H.I., and J.Y.

Data availability
No datasets were generated or analysed during the current study.

Declarations

Ethics approval and consent to participate
Our study was reviewed and approved by the Ethics Committee of University of Occupational and Environmental health.

Consent for publication
Not applicable.

Human Ethics declaration
Not applicable.

Competing interests
The authors declare no competing interests.

Received: 15 August 2024 / Accepted: 29 December 2024
Published online: 09 January 2025

References

1. Zaer H, Glud AN, Schneider BM, et al. Radionecrosis and cellular changes in small volume stereotactic brain radiosurgery in a porcine model. Sci Rep. 2020;10(1):16223.
2. Bijl HP, van Luijk P, Coppes RP, et al. Regional differences in radiosensitivity across the rat cervical spinal cord. Int J Radiat Oncol Biol Phys. 2005;61(2):543–51.
3. Steen RG, Spence D, Wu S, et al. Effect of therapeutic ionizing radiation on the human brain. Ann Neurol. 2001;50(6):787–95.
4. Ohtakara K, Hayashi S, Nakayama N, et al. Significance of target location relative to the depth from the brain surface and high-dose irradiated volume in the development of brain radionecrosis after micromultileaf collimator-based stereotactic radiosurgery for brain metastases. J Neurooncol. 2012;108(1):201–9.
5. Yagi R, Kawabata S, Ikeda N, et al. Intraoperative 5-aminolevulinic acid-induced photodynamic diagnosis of metastatic brain tumors with histopathological analysis. World J Surg Oncol. 2017;15(1):179.
6. Matsuyama T, Kogo K, Oya N. Clinical outcomes of biological effective dose-based fractionated stereotactic radiation therapy for metastatic brain tumors from non-small cell lung cancer. Int J Radiat Oncol Biol Phys. 2013;85(4):984–90.
7. Ohtakara K, Nakao M, Muramatsu H, et al. Nineteen-month immunity to adverse radiation effects following 5-fraction re-radiosurgery with 43.6 gy for local progression after prior 3-fraction radiosurgery for brain metastasis from pan-negative lung adenocarcinoma. Cureus. 2023;15(10):e46374.
8. Ohtakara K, Kondo T, Obata Y, et al. Five-fraction radiosurgery using a biologically equivalent dose of a single fraction of 24 gy for a 3-cm parasagittal paracentral sulcus brain metastasis from adenocarcinoma of the cecum. Cureus. 2023;15(11):e48799.
9. Lin NU, Lee EQ, Aoyama H, et al. Response assessment criteria for brain metastases: proposal from the rano group. Lancet Oncol. 2015;16(6):e270–278.
10. Kim YJ, Cho KH, Kim JY, et al. Single-dose versus fractionated stereotactic radiotherapy for brain metastases. Int J Radiat Oncol Biol Phys. 2011;81(2):483–9.
11. Saitoh J, Saito Y, Kazumoto T, et al. Therapeutic effect of linac-based stereotactic radiotherapy with a micro-multileaf collimator for the treatment of patients with brain metastases from lung cancer. Jpn J Clin Oncol. 2010;40(2):119–24.
12. Choi S, Hong A, Wang T, et al. Risk of radiation necrosis after stereotactic radiosurgery for melanoma brain metastasis by anatomical location. Strahlenther Onkol. 2021;197(12):1104–12.
13. Sneed PK, Mendez J, Vemer-van den Hoek JG, et al. Adverse radiation effect after stereotactic radiosurgery for brain metastases: incidence, time course, and risk factors. J Neurosurg. 2015;123(2):373–86.
14. Minniti G, Clarke E, Lanzetta G, et al. Stereotactic radiosurgery for brain metastases: analysis of outcome and risk of brain radionecrosis. Radiat Oncol. 2011;6:48.
15. Tsuruda JS, Kortman KE, Bradley WG, et al. Radiation effects on cerebral white matter: Mr evaluation. AJR Am J Roentgenol. 1987;149(1):165–71.
16. Furuse M, Nonoguchi N, Kawabata S, et al. Delayed brain radiation necrosis: pathological review and new molecular targets for treatment. Med Mol Morphol. 2015;48(4):183–90.

Publisher's note